CHAPTER II

OZONE FORMATION: PRESSURE DEPENDENCE

2.1 INTRODUCTION

The mass independent (anomalous) oxygen isotopic composition of stratospheric ozone was discovered in 1981 (Mauersberger, 1981). As stated earlier, in the last two decades many isotopic measurements of stratospheric ozone have been carried out in both *in-situ* and stratospheric return samples (Mauersberger, 1981; Mauersberger, 1987; Goldman et al., 1989; Schueler et al., 1990; Mauersberger et al., 1993, 2001; Krankowsky et al., 2000) as well as by spectroscopic means (Rinsland et al., 1985; Abbas et al., 1987; Meier and Notholt, 1996; Irion et al, 1996). A number of laboratory experiments were also performed by different groups (Thiemens and Heidenreich, 1983; Thiemens and Jackson, 1987, 1988, 1990; Morton et al., 1990; Mauersberger et al., 1999), to understand the anomalous behavior of oxygen isotopes in ozone. The present chapter deals with some of the basic aspects of isotopic enrichment in ozone during laboratory study of ozone formation.

2.1.1 Laboratory Experiments

The first laboratory experiment demonstrating heavy oxygen isotopic enrichment in ozone was by Thiemens and Heidenreich (1983). They showed that during the ozone formation by electrical discharge on molecular oxygen (at LN_2 temperature), large mass independent ($\delta^{17}O = \delta^{18}O$) isotopic enrichment (~ 80 ‰) takes place. Thiemens and Jackson (1987, 1988) later showed that ozone produced from UV photolysis of molecular oxygen also has a mass independent heavy isotopic composition. They reported an enhancement of ~ 90 ‰ in both ^{18}O and ^{17}O containing ozone isotopomers.

Morton et al. (1990) investigated the pressure (in the range 5 – 1000 torr) and temperature (in the range 127-360 K) dependence of the isotope ratio produced in the gas phase O (^3P) + O_2 ($^3\Sigma_g$) recombination reaction using visible light (500 – 700 nm) dissociation of ozone to supply O-atom in order to exclude any unknown isotope effect related to excited electronic states of oxygen. They found that the enrichment in ^{18}O and ^{17}O are approximately constant from 5 – 100 torr and decreases at higher pressures in a mass independent fashion ($\delta^{17}O \approx 0.9 \times \delta^{18}O$). Their study also shows that the enrichment increases with increasing temperature with $^{50}O_3$ showing a slightly faster rate of increase than $^{49}O_3$.

Thiemens and Jackson (1990) also investigated the pressure dependency of isotopic enrichment in ozone using UV photolysis of oxygen from 0.8 – 87 atm. They

noted an enrichment (in $\delta^{18}O$) of 90 ‰ at a pressure of 0.8 atm to 10 ‰ at 35 atm. The effect of pressure is less in the range of 45 to 87 atmospheres. Their experiment differs from that of Morton et al. (1990) in the procedure of final ozone production since Morton et al. (1990) produced initial ozone in an electrical discharge, mixed it with oxygen and subsequently photolyzed the mixture in visible light. Figure 2.1 gives the variation of isotopic enrichment with pressure obtained by these two sets of studies (Thiemens and Jackson, 1988, 1990; Morton et al., 1990).

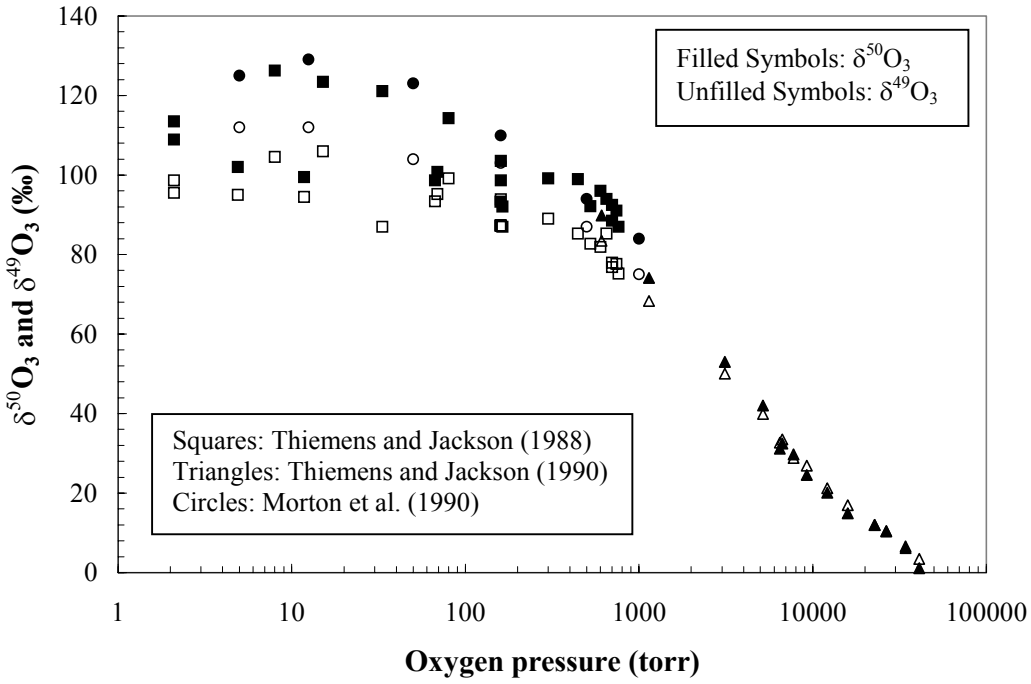

Figure 2.1. *Pressure dependency of isotopic enrichment in ozone (compiled data from different laboratories).*

2.1.2 Motivation Behind the Present Experiment

The present work was undertaken to further explore the ozone isotope enrichment phenomenon in UV photolysis of oxygen by varying ambient oxygen pressure in an effort to understand the variation in isotopic enrichment of stratospheric ozone as described in Chapter I (§ 1.4).

The experiments so far performed in different laboratories were with the basic goal of understanding the non mass-dependent effect itself (as described in § 2.1.1). None of the experiments were specifically planned to address the stratospheric case.

The present experiment was planned to mimic the stratospheric condition as close as possible. In the stratosphere, the photolysis of oxygen occurs in the Schumann-Runge

band (175-200 nm) system, which is the first step of Chapman reaction to form ozone. An important phenomenon in the stratospheric scenario is the recycling (formation as well as dissociation) of ozone for a number of times. The photo-dissociation of ozone in this altitude is mainly by Hartley band (200 – 320 nm) of UV spectrum. It is true that Morton et al. (1990) considered ozone recycling in their laboratory studies. However, since their goal was to study the enrichment in ozone from recombination of ground state oxygen (molecular and atomic) species, they performed the experiment in the Chappuis band (500 – 700 nm). The dynamics associated with the ozone dissociation process in the Hartley band and Chappuis band are different (Valentini et al., 1987). With a motivation for stratospheric applications, the present experiment was carried out in the Hartley band.

In the altitude range of 22 to 33 km constituting the important zone of ozone formation, the total pressure variation is from about 36 to 6 torr (corresponding oxygen partial pressure variation is from about 8 to 1 torr), which is quite large compared to the temperature variation (220 – 228 K). Experimentally it is not feasible to perform the experiment in the pressure range similar to that of the stratospheric oxygen partial pressure due to limitations imposed by surface processes. Therefore, a high-resolution pressure dependence study was planned corresponding to the stratospheric total pressure regime. In this respect, this is the first experimental effort to study some relevant factors related to the stratospheric ozone enrichment phenomenon.

2.2 ABOUT THE EXPERIMENT

The previous experiments dealing with the pressure dependence of ozone isotopic enrichment were aimed at delineating the variation in the primary formation process. In the present case, the formation and dissociation were both permitted to operate simultaneously i.e. the product ozone was not isolated from the photolysis zone by freezing with LN_2. Also, the UV photolysis was done using wavelengths close to the stratospheric window where ozone dissociation is most significant.

2.2.1 Experimental Configuration

Vacuum Manifold and Reaction Chamber:

Figure 2.2 shows the schematic diagram of the vacuum line setup. The line is made of pyrex tubing with greaseless glass stopcocks. A vacuum of < 1 mtorr was achieved by two stages of pumping: mechanical and diffusion pumps. A 5-liter spherical

pyrex chamber (made opaque with aluminum foil) with a MgF_2 side window (1 mm thick and 2 cm diameter) and a cylindrical cold trap at the bottom was used for making ozone from ultra-pure oxygen at different pressures.

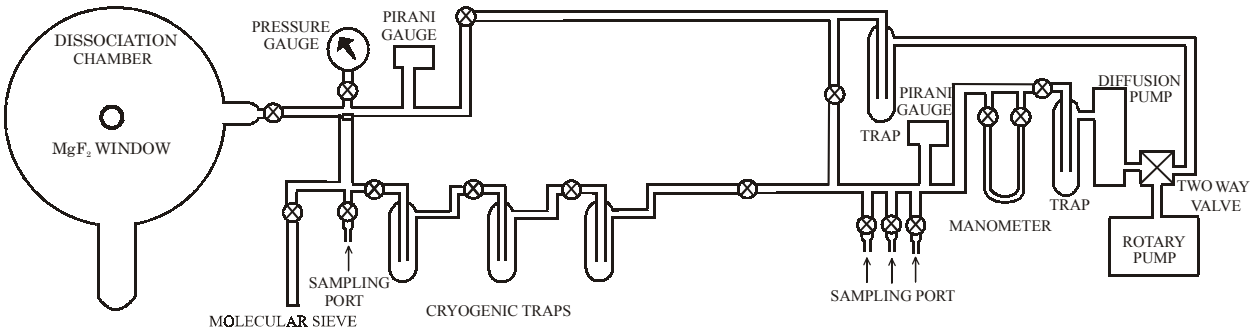

Figure 2.2*. Schematic diagram of the vacuum manifold and reaction chamber used in the experiment.*

UV Light Source:

The UV light is generated by two different electrode-less low pressure (~ 5 torr) lamps, (i) Mercury (Hg), and (ii) Krypton (Kr), excited by a 200 Watt, 2450 MHz microwave generator (Opthos Inc., Model: MPG-4M) coupled to Broida and Evenson cavity respectively. The significant lines, within the UV window of interest, for Hg lamp are 184.9 (1000) and 253.7 (15000) nm and that of Kr lamp are 116.5 (200) and 123.6 (650) nm (the number in the parenthesis denotes the relative strength of each line). The 116 nm line of Kr falls in the fall-off region of transmission curve of MgF_2 window. So, for Kr lamp along with 123 nm, about 80 % of 116 nm enters the reaction chamber.

2.2.2 Experimental Procedure

Ozone dissociation is an integral part of ozone formation (Equations 1.7 to 1.10). To decouple these two effects two sets of experiments were carried out: firstly to study the combined effect of formation and dissociation and secondly to analyze the effect of UV dissociation alone.

In the first set (set 1) of experiment, ultra-pure oxygen (XL grade BOC Gas, 99.99% purity) was photolyzed at pressures from ~10 to 700 torr without removal of product ozone. In order to check the effect of photon energy on the fractionation processes, photolysis was done using two different UV sources, Hg and Kr resonance lamps. Oxygen pressure was monitored by a dial gauge (Figure 2.2). Photolysis was done

for duration of 60 to 1200 minutes depending upon the pressure to produce adequate amount of ozone for mass spectrometric measurement.

In all the second set (set 2) of experiments, ozone was initially formed by photolysis of oxygen at a pressure of 240 torr. Ozone was trapped by LN_2 at the bottom of the chamber and the oxygen pressure was reduced to 1/2, 1/4 and 1/8 in three different cases and the trapped ozone was released. Subsequently, photolysis of the mixture was carried out by the Hg lamp for 8 minutes.

In all cases, the ozone was separated by first condensing it with LN_2 and pumping away the oxygen until a few mtorr pressure was obtained. Subsequently, the LN_2 was removed and ozone was transferred to a second trap with molecular sieve cooled by LN_2. Warming this trap to room temperature converted ozone to oxygen.

All the stable isotopic measurements were performed in VG 903 (Upgrade) and Europa Scientific GEO 20-20 isotope ratio mass spectrometers (IRMS). Ozone samples are converted to oxygen and measurements are done as oxygen. Unless otherwise stated, all the oxygen isotopic measurements reported here are with respect to a laboratory working gas (oxygen) with $\delta^{17}O = 12.48$ ‰ and $\delta^{18}O = 24.58$ ‰ with respect to SMOW with an overall estimated uncertainty (based on a few repeat measurements) of ± 0.1 and ± 0.2 ‰ respectively for $\delta^{18}O$ and $\delta^{17}O$.

To measure small amount of oxygen in VG 903 machine, a cold finger of 0.7 cc (made of stainless steel) with molecular sieve was added at the inlet. During measurement, oxygen samples were completely transferred to this finger from the sample bottle with LN_2. The current in the mass-spectrometer was adjusted near the typical value ~ 10 nA by using different inlet volume of the mass-spectrometer.

To measure the yield of the product ozone (as oxygen), the major beam of the mass spectrometers was used. For GEO 20-20, beam 32 was calibrated with known amounts of oxygen taken in a sample bottle of 1 cc containing molecular sieve. The yield was estimated from the beam 32 strength (all the sample bottles are of the same volume of 1 cc) using the calibration curve. The procedure followed for VG 903 machine is the following: Beam 32 was calibrated with known amounts of oxygen transferred completely into the finger containing molecular sieve (with LN_2). The yield was estimated from the mass 32-beam strength using the calibration curve. To make sure that the calibration curve did not change, along with each sample set a known amount of tank

oxygen was measured and the current was noted after stabilization of the beam. No significant change in calibration was observed during the course of the experiment.

2.3 RESULTS

Experimental results for the first set showing pressure dependence of enrichment are given in Table 2.1 and 2.2 for Hg lamp and Kr lamp respectively. In Figure 2.3 and 2.4, $\delta^{18}O$ and $\delta^{17}O$ of ozone is plotted against the oxygen pressure for Hg and Kr lamp photolysis respectively. The plots show that initially the $\delta^{18}O$ and $\delta^{17}O$ increase gently with decreasing pressure till about 50 torr. Subsequent decrease of pressure is associated with a sharp increase of $\delta^{18}O$ and $\delta^{17}O$ leading to a peak value of 150.1 and 123.5 ‰ at 16 torr oxygen pressure for Hg lamp. Similar nature was observed for the Kr lamp photolysis with the peak values of 147.6 and 114.1 ‰ for $\delta^{18}O$ and $\delta^{17}O$ at 14 torr pressure.

Results for the second set of experiments, UV dissociation of ozone in the presence of oxygen as bath gas at different pressures, are shown in Table 2.3. The result shows that the photolysis of ozone enriches the leftover ozone pool as shown in Figure 2.5 (a). The ozone reservoir enriches by about 22 ‰ when the extent of dissociation is 66 %. In order to determine the fractionation factor α, we assume a Rayleigh model of the form $R = R_o f^{(\alpha-1)}$.

Here R_o is the initial $^{18}O/^{16}O$ ratio of O_3 and R is the same at a given time; f is the fraction of O_3 left after dissociation at that time. Writing in δ notation and taking the natural logarithm we get the following equation:

$$\ln(1 + 0.001 \times \delta) = \ln(1 + 0.001 \times \delta_o) + (\alpha - 1) \ln(f) \qquad (2.1)$$

Where δ_o and δ are the $\delta^{18}O$ of initial ozone and that at a time t respectively.

Figure 2.5 (b) shows the plot of $\Delta\ln(1 + 0.001 \times \delta)$ against ln(f), where Δ is the difference of ln-functions consisting final and initial $\delta^{18}O$ (i.e. $\ln(1 + 0.001 \times (\delta^{18}O)) - \ln(1 + 0.001 \times (\delta^{18}O)_o)$). The best fit of all the data points gives the instantaneous fractionation factor, $\alpha = 1.0192$ for the left-over ozone.

Table 2.1. *Experimental parameters and results for Hg lamp photolysis (set 1)*

Oxygen Pressure (torr)	Exposure Time (min)	Ozone Yield (μmole of O_2)	$\delta^{18}O$ (‰)	$\delta^{17}O$ (‰)	Production Rate (μmole/min)
500.0	155	46.5	91.5	78.0	0.30
336.0	187	39.0	98.6	87.2	0.21
162.0	365	29.0	106.5	89.0	0.079
126.5	410	15.0	109.3	94.2	0.037
50.6	630	15.0	114.1	102.3	0.024
46.8	885	17.0	121.1	103.7	0.019
25.3	870	8.0	126.4	110.3	0.009
18.0	1102	3.4	142.3	118.9	0.003
16.0	1473	2.6	150.1	123.5	0.002
15.0	1140	1.4	134.2	115.5	0.001

Table 2.2. *Experimental parameters and results for Kr lamp photolysis (set 2)*

Oxygen Pressure (torr)	Exposure Time (min)	Ozone Yield (μmole of O_2)	$\delta^{18}O$ (‰)	$\delta^{17}O$ (‰)	Production Rate (μmole/min)
607.2	105	85.0	95.0	78.6	0.810
405.0	120	86.6	101.3	82.5	0.633
175.0	180	101.2	107.1	90.3	0.562
139.0	382	188.7	112.0	93.7	0.523
73.0	180	63.2	116.0	96.0	0.194
43.0	247	60.9	124.7	98.3	0.344
32.0	270	24.3	121.7	98.9	0.222
18.0	330	18.0	135.6	105.9	0.055
16.0	570	23.7	143.6	108.0	0.042
14.0	258	13.0	147.6	114.1	0.050
12.0	874	25.0	129.4	99.6	0.029
12.0	720	21.4	130.0	101.0	0.030
10.0	1920	17.0	136.2	105.9	0.009
8.0	1765	14.0	132.4	102.2	0.008

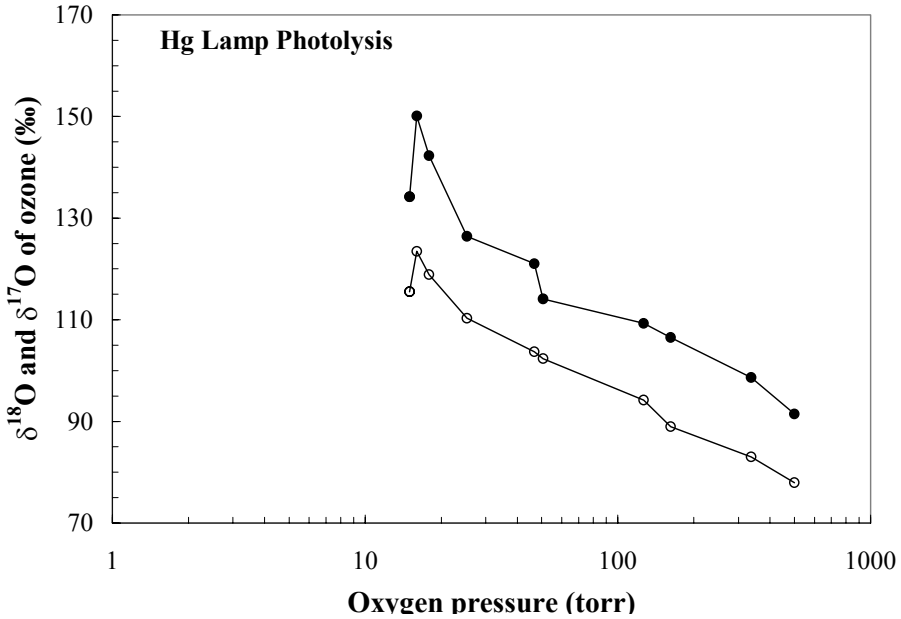

Figure 2.3. *Variation of $\delta^{18}O$ (filled circle) and $\delta^{17}O$ (unfilled circle) of ozone with oxygen pressure from 10 to 550 torr for Hg lamp photolysis. He Error of individual data point is comparable to the size of the symbol.*

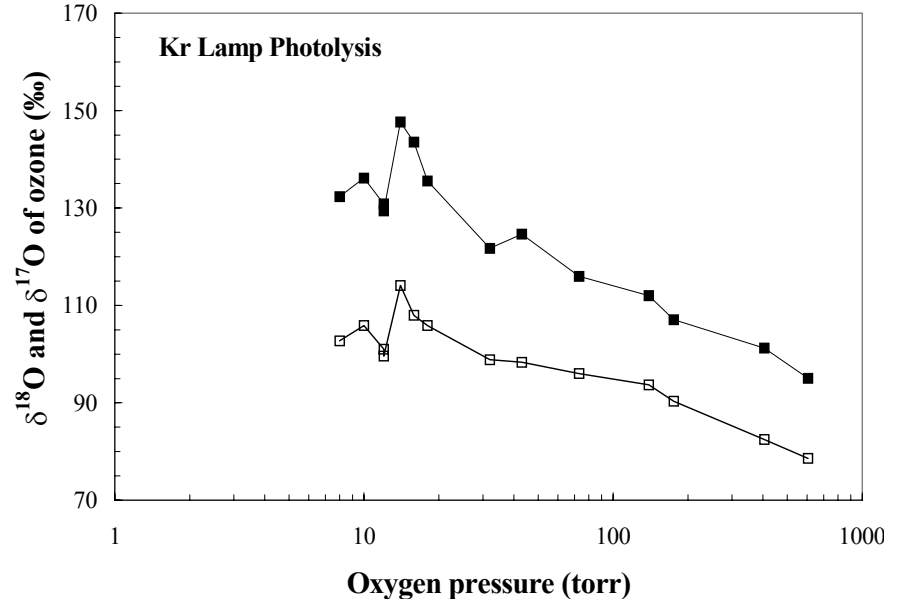

Figure 2.4. *Variation of $\delta^{18}O$ (filled square) and $\delta^{17}O$ (unfilled square) of ozone with oxygen pressure from 8 to 600 torr for Kr lamp photolysis. The error of individual data point is comparable to the size of the symbol.*

Table 2.3. *Experimental parameters and results for UV dissociation of ozone in the presence of bath gas oxygen at different pressures (set 2).*

Initial Ozone Amount (μmole of O_2)	Bath Gas Oxygen Pressure (torr)	Left-over Ozone Yield (μmole of O_2)	$\delta^{18}O$ of Ozone (‰)	$\delta^{17}O$ of Ozone (‰)	Fraction Left
45.0	120	29.8	106.6	112.2	0.66
50.0	60	24.9	111.6	104.7	0.50
56.0	30	21.0	122.0	123.2	0.38
Initial Ozone Composition			99.0	95.3	

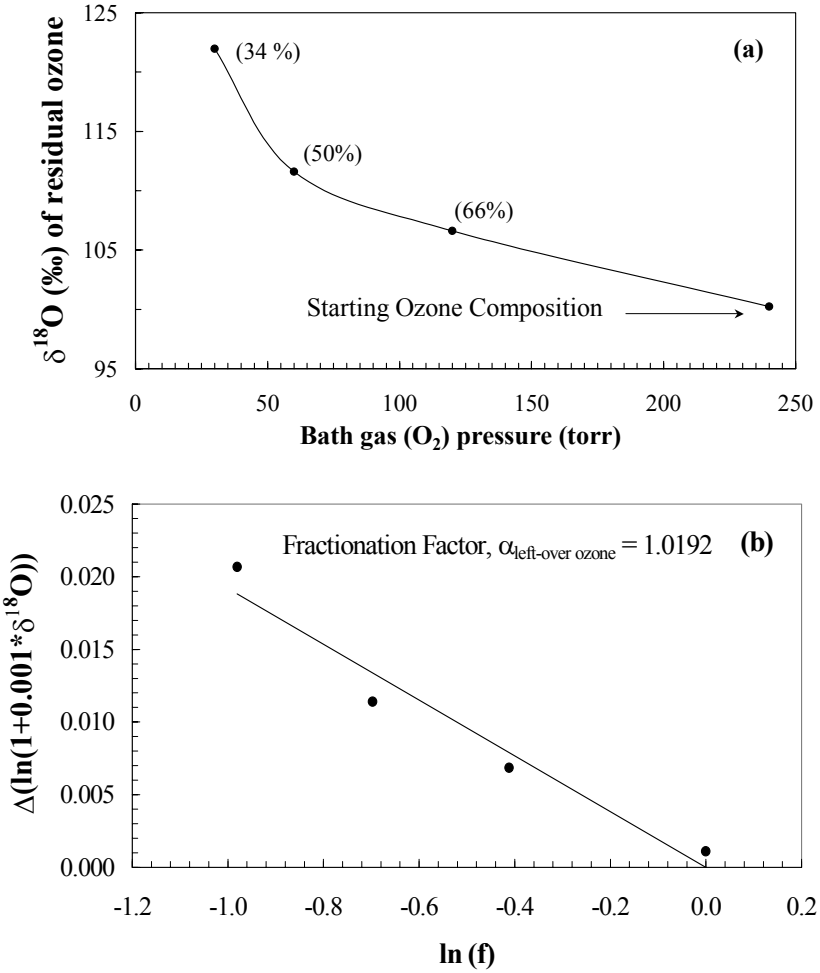

Figure 2.5. *Effect of dissociation on the enrichment process. (a) $\delta^{18}O$ of the leftover ozone after dissociation at three different bath gas oxygen pressures. The bath gas oxygen controls the extent of dissociation during the photolysis time of 8 minutes. Enrichment of 22 ‰ was observed at the dissociation level of 66 %. (b) Plot of Eqn. 2.1 (as described in the text) to calculate the fractionation factor of the dissociation process using a Rayleigh model. The instantaneous fractionation factor is calculated to be 1.0192 for leftover ozone.*

2.4 DISCUSSION

The present results demonstrate that production of ozone through UV photolysis of oxygen is always associated with heavy isotope enrichment and confirm the earlier results (Thiemens and Jackson, 1987, 1988). The $\delta^{18}O$ is above about 80 ‰ for all three types of UV range investigated so far by different workers i.e. resonance Hg (184.9 and 253.7 nm) lamp, Kr lamp in 116 to 160 nm range and Xe continuum lamp in 155 to 180 nm range (present work and Thiemens and Jackson, 1987, 1988). For all the lamps the nature of pressure dependence of $\delta^{18}O$ and $\delta^{17}O$ is the same. This shows that the enrichment process is largely independent of energy of the dissociating photon.

The increase in enrichment with decrease in pressure (Figure 2.4 and 2.5) occurs differently over three pressure ranges: (I) 700 to 50 torr, where the increase of enrichment is gentle, (II) 50 to 15 torr, where the increase is sharp and a peak is observed, and (III) below 15 torr where the enrichment decreases sharply.

The photochemical processes involved in the experiments are as follows (similar to that expressed in § 1.3): (1) primary processes,

$$O_2 + h\nu \rightarrow O + O \qquad (2.2)$$

$$O + O_2 + M \rightarrow O_3 + M \qquad (2.3)$$

and (2) secondary processes,

$$O_3 + h\nu \rightarrow O_2 + O \qquad (2.4)$$

$$O + O_3 \rightarrow 2O_2 \qquad (2.5)$$

In the pressure regime of 50 to 700 torr (Range I), the gentle increase of enrichment with lowering of pressure is also evident from previous laboratory experiments as described in § 2.1.1.

2.4.1 Pressure Dependence in Range I and Gao-Marcus Theory

The gentle increase in enrichment with decrease in pressure has been modeled by Gao and Marcus (2001, 2002) using a novel approach. They have shown that the lower density of states of symmetric molecules can make the collisional energy transfer less efficient and lead to faster dissociation of the symmetric transient ozone complex. Therefore, isotopic enrichment would have inverse pressure dependence. The results in the pressure range of 50 to 500 torr (Range I) can nicely be explained by this mechanism, which demonstrates that in this pressure range primary process of ozone formation

dominantly controls the isotopic enrichment in the product ozone compared to the secondary processes.

2.4.2 Significant Effect of Secondary Processes in Enrichment

The isotopic enrichment pattern in Range II is different from that of Range I (see Figures 2.3 and 2.4). We propose that an additional contribution from the secondary processes (i.e. dissociation of ozone) is responsible for the observed rapid rise in enrichment in the Range II. The additional increase in enrichment in the final product ozone due to dissociation alone is not dealt with by Gao-Marcus theory.

The proposition that dissociation of ozone is responsible for the rapid rise is confirmed by the next set (set 2) of experiments. In this set (set 2) of experiments, photolysis of ozone was carried out along with bath gas oxygen kept at three different pressures. The data shows that (Figure 2.5 (a)) as the bath gas pressure decreases, the extent of dissociation increases. As the other controlling factors which can govern the extent of dissociation, (e.g. photolysis time, amount of initial ozone) are kept constant, it can be argued that different bath gas pressures control the extent of ozone dissociation instead of taking any significant part in ozone formation process. So, during the photolysis time of 8 minutes, the primary process leading to ozone formation is negligible compared to the secondary process of ozone dissociation (since, considering the production rate of 0.037 μmole/min from Table 2.1 for 120 torr oxygen pressure, 8 minutes photolysis can contribute only 0.3 μmole of ozone for the first entry of Table 2.3). In other words, set 2 experiments provide the insight to the ozone dissociation processes. Figure 2.5 (a) shows that the isotopic enrichment increases with the magnitude of dissociation (calculated using the amount of ozone left and the initial amount). For example, if the left-over ozone is 34 % of the original, the isotopic enrichment is about 22 ‰. Applying the calculated fractionation factor (1.0192) to PRL data (experiments carried out at Physical Research Laboratory, India) (17.5 to 50 torr range (Range II) in set 1) it is estimated that 87 % loss of initial ozone is required to obtain an enhancement of the isotopic enrichment by 36 ‰ at 17.5 torr (over a value of 116 ‰ at 50 torr from where the influence of dissociation starts to increase rapidly) assuming no recycling of ozone.

Before discussing the PRL results in more detail it is worthwhile to describe and discuss the results from a similar set of experiments carried out at the University of

California, San Diego (UCSD). The UCSD results and the PRL results together clarify the underlying factors behind the pressure dependency in a complimentary way.

2.4.3 Experimental Results of UCSD

The UCSD experiments are similar to that of the first set (related to ozone formation) described in § 2.2. These experiment were performed in three different configurations. In the first configuration, abbreviated as config. I, ultra pure oxygen was photolyzed at pressures from 6 to 700 torr without removal of product ozone during photolysis; in config. II, product ozone was removed during photolysis (done only at oxygen pressures from 8 to 90 torr) by condensation in the trap; in config. III, a mixture of oxygen and nitrogen was photolyzed at a total pressure of 100 torr, but with variable ratios between them. According to this nomenclature, experiments under PRL set 1 category belong to config. I of UCSD.

Table 2.4. *Experimental parameters and results for Hg lamp photolysis performed at UCSD for three different configurations as described in the text.*

A. Config. I (without removing the product ozone during photolysis)

Oxygen Pressure (torr)	Exposure Time (min)	Ozone Yield (μmole of O_2)	$\delta^{18}O$ (‰)	$\delta^{17}O$ (‰)	Production Rate (μmole/min)
702.0	120	165.2	90.4	84.6	1.4
400.0	124	163.3	100.3	93.0	1.3
100.6	900	128.5	115.3	105.0	0.14
50.0	240	21.9	122.4	112.1	0.09
35.0	240	9.6	130.3	116.8	0.04
25.0	300	1.05	153.2	128.1	0.0035
20.0	240	0.21	169.9	134.7	0.0009
18.0	270	0.09	171.3	136.0	0.0003
17.5	810	0.62	180.7	140.7	0.0008
15.1	1045	0.17	152.0	125.5	0.0002
15.0	780	0.46	138.0	116.8	0.0006
10.0	360	0.56	138.8	116.3	0.0016
8.4	800	0.02	137.0	111.9	0.00002
6.7	765	0.05	115.4	95.4	0.00006

B. Config. II (removing the product ozone during photolysis by LN_2 in the bottom trap)

Oxygen Pressure (torr)	Exposure Time (min)	Ozone Yield (μmole of O_2)	$\delta^{18}O$ (‰)	$\delta^{17}O$ (‰)	Production Rate (μmole/min)
7.9	300	12.8	126.6	113.8	0.90
18.3	180	29.9	115.4	107.6	0.93
25.0	230	38.6	123.3	103.6	0.84
50.7	112	11.2	120.3	109.4	0.91

C. Config. III (without removal of product ozone during photolysis with Nitrogen at 100 torr total pressure)

Oxygen Pressure (torr)	Exposure Time (min)	Nitrogen Pressure (torr)	Ozone Yield (μmole of O_2)	$\delta^{18}O$ (‰)	$\delta^{17}O$ (‰)	Production Rate (μmole/min)
5.0	1230	95.0	0.1	141.9	115.5	0.0001
7.5	1132	92.8	0.2	148.1	119.4	0.0002
10.0	840	90.0	0.4	176.3	133.9	0.0005
11.9	1060	88.1	0.8	167.3	130.3	0.0008
17.9	1110	82.1	6.8	135.5	115.1	0.0061
50.1	180	49.8	16.2	125.7	113.6	0.090

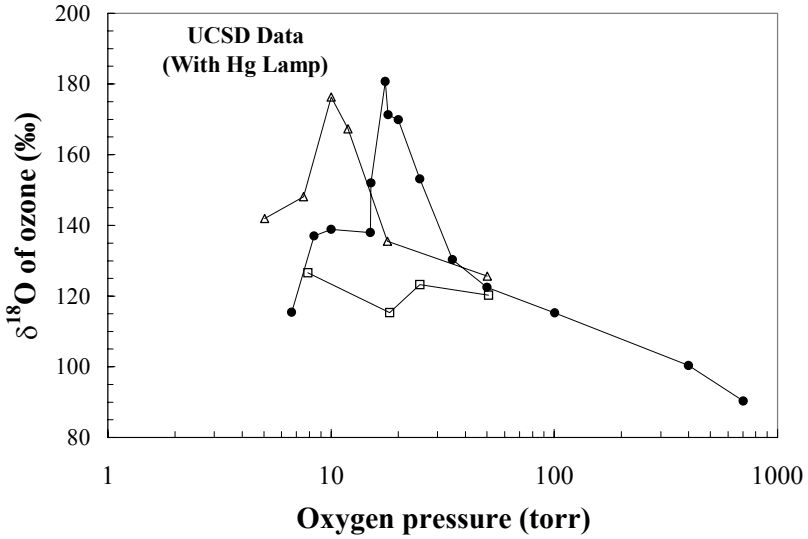

Figure 2.6. *Variation of $\delta^{18}O$ of ozone with oxygen pressure from 6.7 to 700 torr for Hg lamp photolysis in three different configurations performed at UCSD (the symbols circle, square and triangle are for config. I, II and III respectively). Note the absence of peak in config. II experiment, where the formed ozone was trapped as soon as it formed in the bottom finger of the reaction chamber with LN_2. The shift in peak from 17.5 torr to 10 torr is due to addition of nitrogen to the system.*

The results of these experiments are given in Table 2.4. Figure 2.6 shows the variation of $\delta^{18}O$ with pressure from 6.7 to 700 torr. The pattern is similar to that of Figure 2.3 and 2.4 with three distinct pressure ranges. The peak value of enrichment was obtained at a pressure of 17.5 torr with a value of 180.7 ‰ for $\delta^{18}O$. This value is about 30 ‰ higher compared to the peak values obtained in PRL experiments with Hg and Kr lamps (150.1 and 147.6 ‰ respectively). The reason for this apparent discrepancy is explained further on.

2.4.4 Dissociation Effect in the Pressure Range II

The major difference between the config. I and config. II experiments of UCSD is that both the primary and secondary processes are in operation in config. I whereas in config. II, mostly primary processes are operative. Figure 2.6 suggests that the peak in pressure range II vanishes when the secondary process, i.e. the dissociation process, is minimized by ozone absorption. Therefore, in the low pressure regime the dissociation processes act in tandem with the (primary) formation process and contribute significantly to the enrichment. The production rate plot (Figure 2.7) for pressure Range I, II and III (for PRL data) does not show uniform rate of increase with the increase of oxygen pressure; instead, the rate of increase of production rate is slower in Range II. This proves that the effect of dissociation in Range II is more important than Range I in a relative sense. In our experimental set-up, the Kr lamp was found to be more efficient probably due to generation of higher UV flux leading to higher dissociation of oxygen.

Figure 2.8 is the three-isotope plot between $\delta^{18}O$ and $\delta^{17}O$, showing the slopes in three pressures ranges for both the lamps for PRL (set 1) experiments. The proposition that dissociation plays an important role in the 15 to 50 torr range (Range II) is corroborated by the slope values. The slopes in config. I in the pressure Range II for both the lamps are close to that of UV dissociation slope (slope = 0.6, see Chapter III), suggesting that the enrichment in this pressure range is controlled by the photo-dissociation process. The slopes for Ranges I and III show a value close to 1, which is a value for pure ozone formation only by the primary processes (Thiemens and Heidenreich, 1983). So, the enrichment noted above about 100 ‰ can be attributed to the effect of UV dissociation.

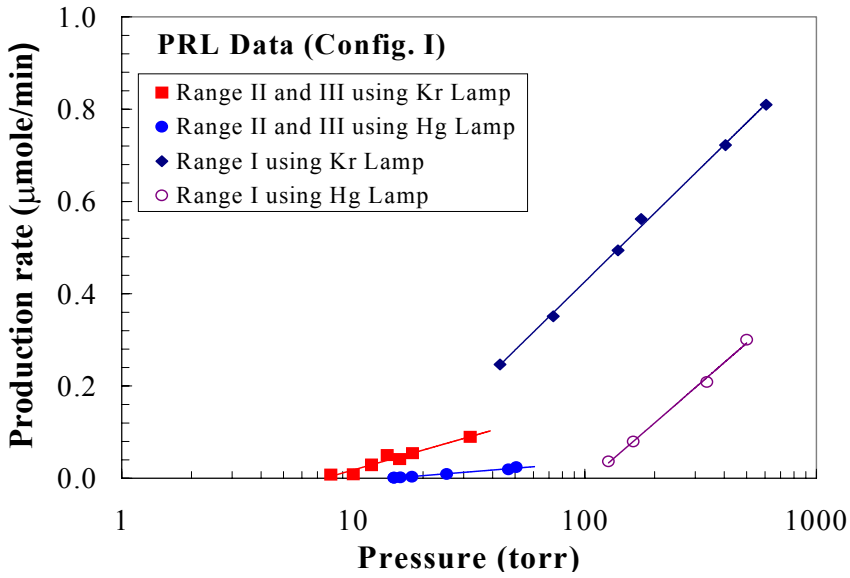

Figure 2.7. *Pressure dependence of production rate for pressure Ranges I (50 to 500 torr), II (15 to 50 torr) and III (8 to 15 torr). The rate of production of ozone for all the ranges is larger for Kr lamp than the Hg lamp photolysis. The production rate increment pattern with increasing pressure for Ranges I and II are not same. The increase in rate is slower in Range II, compared to Range I. This establishes that dissociation of ozone is relatively more important to increase the isotopic enrichment in the low-pressure range.*

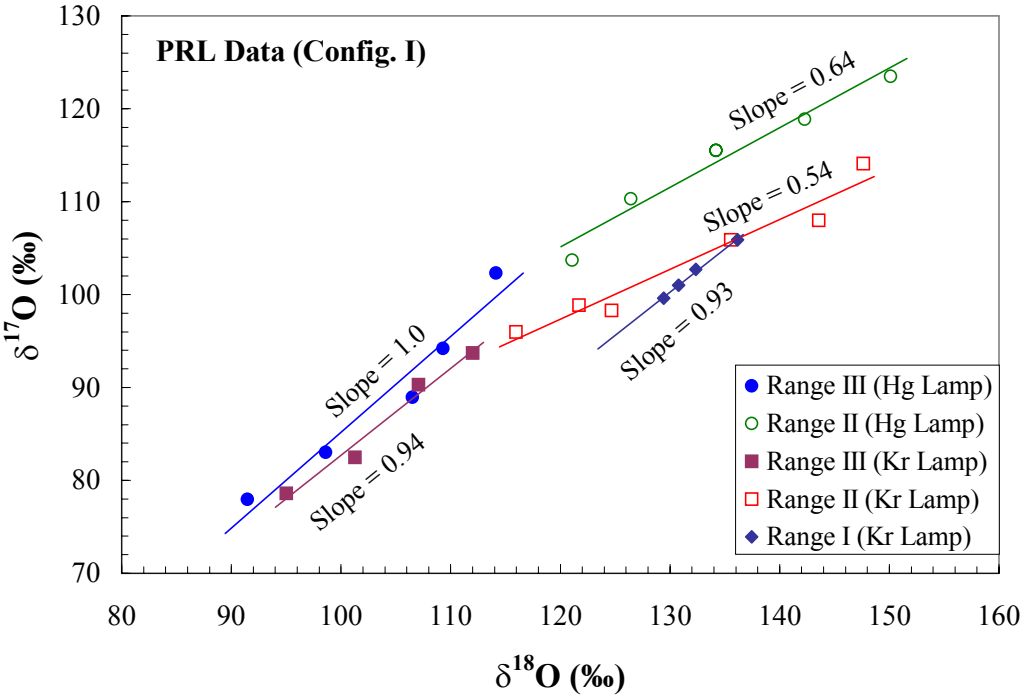

Figure 2.8. *Three-isotope plot of photolysis data for all the three pressure ranges with both the lamps. The slopes of ranges I and III are nearly same for both the lamps (due to less number of points, the data of Range III for Hg lamp photolysis was not plotted). The slopes for Range II for both the lamps have values close to that obtained from ozone dissociation alone.*

2.4.5 Enrichment in Range III

At pressure Range III (below 15 torr) we obtained lower enrichments than the peak zone. Lower values of enrichment with decrease of pressure below ~ 15 torr was observed with a slope of ~ 0.9, which is higher relative to its value (~ 0.6) in the neighboring 15 to 50 torr range (Range II). The cause for this turn-around is still to be explained. One of our recent studies (described in Chapter III) shows that dissociation of ozone on a glass surface enriches the left-over ozone pool in a mass independent (slope = 1) fashion. It is conceivable that in the low-pressure range, the ozone molecules can migrate to the wall of the reaction chamber where surface dissociation of ozone takes place and contributes to increase the slope. However, since surface dissociation is a less efficient process, the magnitude of enrichment is lower than the peak region.

2.4.6 Effect of Nitrogen in the system

In the context of dissociation, it is easy to see how the addition of nitrogen shifts the peak to lower pressures (config. III, UCSD data). As explained above, the peak is the result of significant UV dissociation of ozone in a dynamic sense. The net amount of ozone is determined by the integrated rate of production and destruction. At equilibrium, these two rates are equal and the reservoir amount is constant. The role of dissociation at this stage is essentially recycling the ozone at a fixed rate. The relative strength of the reservoir, vis-à-vis the dissociation rate, gives a measure of the turn-over time ($\tau = [O_3] / d[O_3]/dt$, where $[O_3]$ is the ozone amount at a given time and $d[O_3]/dt$ is the dissociation rate at that time), whose value determines the position of the peak i.e. the peak develops when the net amount of ozone over dissociation rate is below a critical level determined by UV flux, transmission and oxygen pressure. Addition of nitrogen increases the collision frequency and results in a larger amount of ozone being formed which has the effect of increasing the value of τ (relative to the case when only oxygen is present at the same partial pressure). Therefore, the same peaking effect is seen at lower oxygen partial pressure when the value of τ is reduced again below the critical level. This observation provides another support to our proposition involving the turn-over time.

2.4.7 Amount Dependence in Enrichment of Ozone

As mentioned before, the enrichment noted at UCSD with similar set-up and experimental configuration was higher compared to that of PRL in the pressure Range II.

We note that the ozone yield of UCSD experiments were below 1 μmole in the pressure Range II whereas the yield of PRL experiments were around 10 μmole or more (except for two data points of Hg lamp photolysis) in the same pressure range (compare Tables 2.1 and 2.2 with Table 2.4A). To explore the amount dependence of enrichment another set of experiments was performed.

Table 2.5. *Experimental parameters and results showing amount dependence of enrichment. Table A and B are for Kr lamp photolysis for initial oxygen pressure of 74 and 32 torr and Table C is for Hg lamp photolysis at 200 torr initial oxygen pressure.*

A. Initial oxygen pressure of 74 torr (Kr Lamp)

Exposure Time (min)	Ozone Yield (μmole of O_2)	$\delta^{18}O$ (‰)	$\delta^{17}O$ (‰)	Production Rate (μmole/min)
17	0.7	136.6	96.1	0.04
30	4.1	123.6	99.1	0.14
45	9.1	118.1	82.8	0.20
60	12.7	114.7	78.6	0.22
90	20.5	114.5	88.7	0.23
180	35.0	115.9	98.0	0.19
300	53.8	116.3	83.0	0.18

B. Initial oxygen pressure of 32 torr (Kr Lamp)

Exposure Time (min)	Ozone Yield (μmole of O_2)	$\delta^{18}O$ (‰)	$\delta^{17}O$ (‰)	Production Rate (μmole/min)
30	2.6	139.1	101.9	0.09
45	8.0	123.5	85.7	0.18
90	13.4	122.0	79.6	0.15
270	60.0	121.7	98.9	0.22

C. Initial oxygen pressure of 200 torr (Hg Lamp)

Exposure Time (min)	Ozone Yield (μmole of O_2)	$\delta^{18}O$ (‰)	$\delta^{17}O$ (‰)	Production Rate (μmole/min)
25	1.7	109.9	115.6	0.07
30	3.6	100.4	116.8	0.12
38	6.2	97.5	115.5	0.15
50	9.5	96.0	115.9	0.19
70	15.0	96.0	115.0	0.21
110	34.4	94.9	112.7	0.31

Ozone was formed by photolysis of oxygen kept at a fixed pressure. The photolysis time was varied and different amount of ozone was produced. Each time the product ozone was collected and its amount and isotopic composition were measured (procedure described in § 2.2). The experiment was done for 74 and 32 torr of oxygen pressure using Kr lamp and at 200 torr oxygen pressure with Hg lamp. The experimental results are given in Table 2.5.

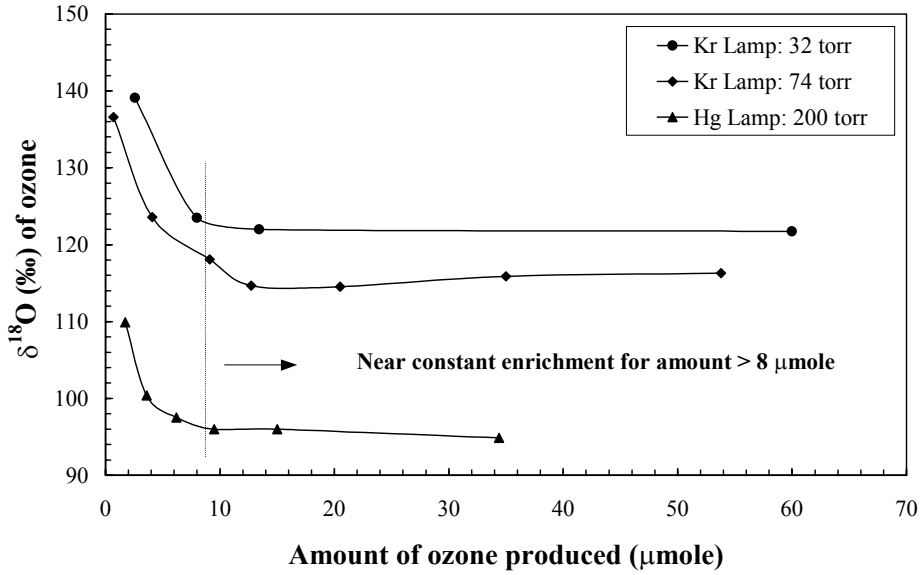

Figure 2.9. *Isotopic enrichment in ^{18}O with the amount of ozone produced (by varying the photolysis time) for three different pressures. When the production is less that ~8 μmole, enrichment increases with decreasing amount for all the three pressures. Beyond 8 μmole the enrichment is almost constant. The uncertainty in each data point is comparable to the size of the symbol.*

Figure 2.9 shows isotopic enrichment in ^{18}O with the amount of ozone produced (by varying the photolysis time) for three different pressures. When the production is less than ~ 8 μmole, enrichment increases with decreasing amount for all the three pressures. In contrast, beyond an ozone amount of ~ 8 μmole, the $\delta^{18}O$ is almost constant. In the constant enrichment zone, the pressure dependence of enrichment is also evident. The enrichment for 32 torr is higher than the enrichment for 74 torr, which in turn is higher than that for 200 torr.

The amount dependency of enrichment can explain the discrepancy in the magnitude of enrichment in the peak zone between UCSD and PRL results. In the pressure Range II, for UCSD experiments, the yield of ozone was about one μmole or less (for 25 torr and below). This contributes additional enrichment due to the amount effect.

For PRL experiments, when Kr lamp was used for photolysis, the yield for the same pressure range was much more than the transition value of ~ 8 μmole. For Hg lamp photolysis, in the same pressure range for two pressures 17.9 and 16.0 torr, the yield was ~ 3 μmole and for others it was more than 8 μmole. The enrichment noted for these two pressures also show little higher value compared to the enrichment observed for Kr lamp in the nearby pressures (Tables 2.1, 2.2 and 2.4A). In order to detect the pressure effect alone, it is therefore important to maintain the ozone yield above 8 μmole as done for most of the PRL experiments.

2.5 CONCLUSION

The pressure dependency of enrichment of heavy oxygen isotopes in ozone was studied in the pressure zone relevant to stratospheric pressure with high resolution. Stratospheric conditions were maintained as close as possible regarding the UV energy window and ozone recycling (primary and secondary processes were allowed to take place simultaneously).

It is observed that depending upon heavy oxygen isotopic enrichment pattern, the examined pressure zone can be divided into three ranges. Beyond 50 torr pressure (Range I), the enrichment in ^{17}O and ^{18}O decreases gently with increasing pressure. Within 50 to 15 torr (Range II), enrichment increases sharply with decreasing pressure. Again below 15 torr (Range III), enrichment decreases with decreasing pressure. The three-isotope plot depicts different slopes (between $\delta^{17}O$ and $\delta^{18}O$) in these three pressure ranges. The slopes in Ranges I and III are close to unity whereas the slope in Range II is close to 0.6. It was shown that dissociation of ozone (as a secondary process) plays an important role in pressure range II, which brings down the slope close to 0.6 from unity. Considering simultaneous formation and dissociation, a parameter called turn-over time (τ) is introduced to explain the enrichment pattern in pressure range II. The transition of slope from 0.6 to unity again in pressure range III is attributed to the surface effect. Some of these results can be applied to the stratosphere to explain the altitudinal variation of enrichment and will be discussed in Chapter V.